



ELSEVIER

Contents lists available at SciVerse ScienceDirect

## Microelectronics Journal

journal homepage: [www.elsevier.com/locate/mejo](http://www.elsevier.com/locate/mejo)

## Data bus swizzling in TSV-based three-dimensional integrated circuits



Shen Ge\*, Eby G. Friedman

Department of Electrical and Computer Engineering, University of Rochester, Rochester, NY, USA

## ARTICLE INFO

## Article history:

Received 29 August 2012

Received in revised form

10 May 2013

Accepted 13 May 2013

Available online 12 June 2013

## Keywords:

Data bus

Swizzling

Through silicon via

Three-dimensional integrated circuits

## ABSTRACT

The purpose of this paper is to efficiently exploit swizzling in reducing coupling noise between the bit lines of a TSV-based data bus in three-dimensional integrated circuits. The core concept of swizzling is to distribute the noise of an aggressor to all victims, rather than concentrating on the nearest victim. Based on this principle, an optimal swizzling pattern, which achieves an equal distribution of the coupling impedance, is proposed. The efficiency of this optimal pattern is demonstrated through comparison to no swizzling and two other swizzling patterns while considering different TSV diameters, aspect ratios, pitches, and transition times of the aggressor signal. A circuit model of a TSV-based 3-D data bus is evaluated in HSPICE with each TSV modeled as an RLC impedance. A maximum reduction of 51% in peak coupling noise is achieved.

© 2013 Elsevier Ltd. All rights reserved.

## 1. Introduction

With the increasing need for high performance electronic devices, the semiconductor industry is integrating more modules onto an integrated circuit (IC) [1]. The area of a single die therefore keeps growing, increasing the length of the long interconnects. One severe consequence of this issue is the effect on the data bus.

A data bus carries data to communicate among the CPU, caches, lower level memory, and peripherals. The CPU latency and memory bandwidth can be significantly affected by the length and width of a data bus [2]. Increasing the length and decreasing the distance between bit lines of a data bus increases the parasitic coupling impedance, characterized by the fringing capacitance and mutual inductance. A fast switching line can affect the signal integrity of adjacent bit lines, which is known as crosstalk [3]. Misinterpretation of a signal can occur if the induced coupling noise on the victim lines is sufficiently large. A high amplitude and long lasting noise signal can dissipate extra power via glitches [4], thereby producing more heat [5], which exacerbates the high heat density already existing in integrated circuits [6,7]. The influence of capacitive and/or inductive coupling on signal integrity is therefore important. Several methods to reduce coupling effects have been proposed, such as wider lines, longer distances, and shielding [8–12]. More metal or a larger area, however, is required by these techniques. Hence, there is a need for design techniques that will enhance data bus performance such as power efficiency and high speed with small area.

Three-dimensional integrated circuits (3-D ICs) are a promising circuit technique. A 3-D IC is a stacked structure of 2-D ICs. The

advantages of a 3-D IC include (a) parallel processing, (b) smaller area with shorter horizontal interconnects, (c) functional and technological heterogeneity, (d) lower power, and (e) higher speed [1,5]. To achieve these advantages, a highly efficient data bus is necessary to guarantee the speed and accuracy of the inter-layer communication.

Vertical communication among the multiple layers within a 3-D IC generally utilizes wire bonds, bumps, and through silicon vias (TSVs) [13]. A TSV is a cylinder shaped connection, categorized as either a bulk TSV or a thin film TSV with respect to the thickness of the substrate. As shown in Fig. 1,  $D$  is the diameter of the TSV cross-section, the aspect ratio ( $AR$ ) of a TSV is the length over the diameter, and the pitch ( $P$ ) is the summation of one TSV diameter ( $D$ ), one spacing ( $S$ ), and twice the barrier thickness. As compared to other connections such as wire bonds, a TSV requires less area, which reduces the package volume. Signal reflections due to impedance mismatches are less significant in a continuous TSV-based signal path than a bump-based signal path [14,15]. TSVs are expected to greatly expedite vertical communication among 3-D layers.

The increasing length of a TSV-based 3-D data bus can result in greater crosstalk. Swizzling, inspired by twisted pair cables, is proposed to reduce coupling noise while satisfying the limitations of metal and area. Swizzling is a method to reduce coupling by changing the frequency of adjacency between the same two bit lines [16,17]. The influence of an aggressor line is distributed to the other bit lines rather than concentrate on the closest bit line. The performance of a parallel data bus is determined by the worst case bit line, either the line with the largest delay or highest noise. As shown in Fig. 2, the bit line closest to the aggressor line is described as the *victim* while the farther bit lines are regarded as *refugees*. The refugee lines are less affected by coupling from an aggressor due to the farther distance, while swizzling requires each refugee line to temporarily become a victim. Coupling effects on refugee lines,

\* Correspondence to: 7300 RR 2222, Building I, SARC, Austin, TX 78730, USA. Tel.: +1 585 727 1606.

E-mail addresses: [shen.ge@rochester.edu](mailto:shen.ge@rochester.edu), [geshen1989@gmail.com](mailto:geshen1989@gmail.com) (S. Ge).

which are considered as local coupling, are therefore increased. But as the victim is not fixed to one specific bit line, the worst case noise is less. The maximum noise observed at the output of a swizzled data bus, which is considered as global coupling, is therefore reduced.

As shown in Fig. 3, a swizzled data bus consists of horizontal and vertical paths. The total length of each rerouted signal path can be longer, but the delay is not necessarily greater as the speed is determined by the impedance of the entire path. In a parallel data bus without swizzling, the speed and signal integrity of the victim bit line next to the aggressor is affected the greatest. The influence of the aggressor on the non-adjacent victims decreases with increasing distance. The performance of a parallel data bus is however limited by the worst case bit line. If the influence of the aggressor is distributed to every victim, rather than concentrated on one victim,

the performance of all of the victim bit lines will be the same. The worst case scenario is then avoided. In this paper, the optimal swizzling pattern is the configuration in which the peak coupling noise is minimized. An intuitive assumption of optimal swizzling is described as follows: if the impedance of all of the signal paths is the same, each bit line other than the aggressor can temporarily be a victim and is a refugee at all of the other times. The situation in which no bit line is a victim *all of the time* improves the signal integrity of the overall data bus. If the impedance of all of the signal paths is the same, the entire delay along each signal path is also the same (assuming the drivers and loads are the same). The speed of a data bus is therefore not limited by the slowest bit line. The objective of optimal swizzling of a TSV-based 3-D data bus is to evenly distribute the coupling impedance of every bit line.

This paper is organized as follows: the optimal swizzling pattern is described in Section 2. Swizzling is evaluated, considering different TSV diameters, aspect ratios, pitches, and aggressor switching speeds, in Section 3, and the efficiency of swizzling based on HSPICE simulation is also reviewed in Section 3. This paper is concluded in Section 4.

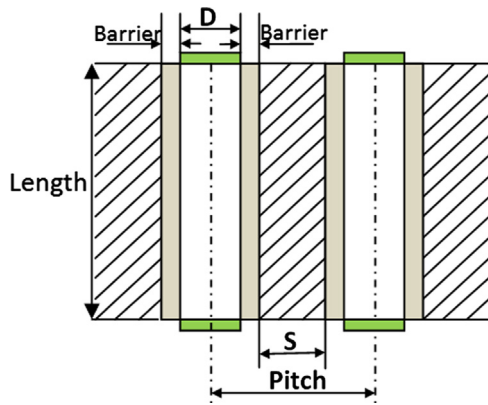


Fig. 1. Dimensions of a TSV.

## 2. Optimal swizzling

Each swizzling event, where the direction of the path is changed, can occur at the end of each TSV rather than at the middle. Hence, swizzling a TSV-based 3-D data bus is limited by the number of planes within a 3-D system. A swizzled data bus consists of vertical and horizontal paths. For a wide data bus, 64 or more bits, the horizontal impedance becomes more significant since the horizontal length is comparable to the vertical distance. The horizontal

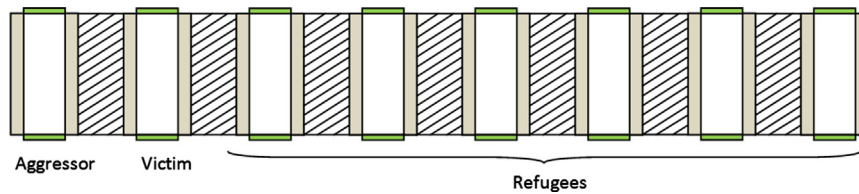


Fig. 2. Aggressor, victim, and refugees in a TSV-based 3-D data bus.

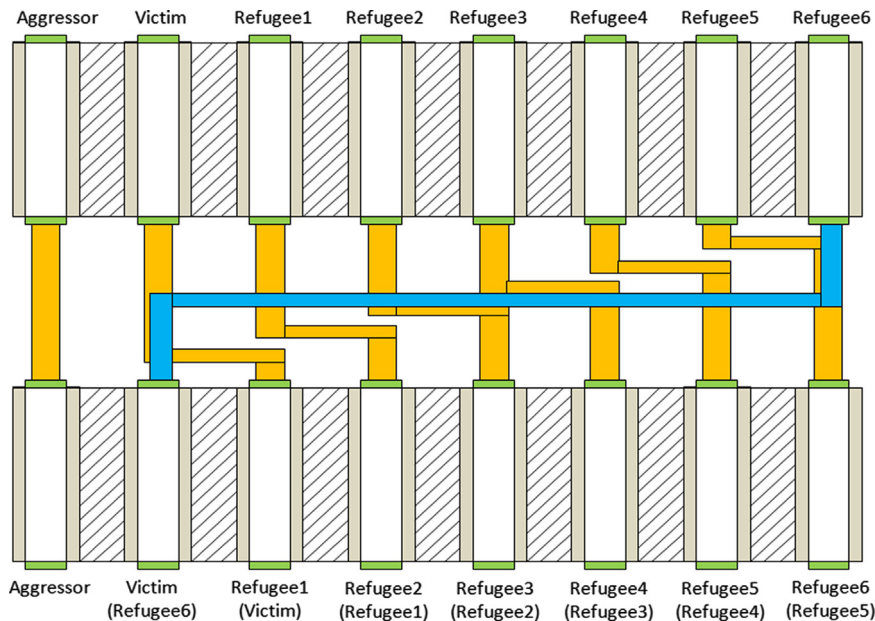


Fig. 3. A swizzled TSV-based 3-D data bus.

impedance of an eight bit data bus is neglected in the HSPICE circuit model since the horizontal length is relatively short.

The optimal swizzling pattern considers the impedance of each bit line. As shown in Fig. 4, the parasitic impedance is characterized by the resistance  $R_{self}$ , capacitance, and inductance [18]. The capacitance consists of the self-capacitance  $C_{self}$  and coupling capacitance  $C_c$ , while the inductance consists of the self-inductance  $L_{self}$  and mutual inductance  $L_m$ . To determine the impedance of each individual signal path, the bit lines are initially decoupled. As shown in Fig. 5, this process is based on the decoupling technique described in [19,20], where, for the aggressor, the decoupled self-capacitance is  $C_{self}$  and the self-inductance is  $L_{self}+L_m$ , while for the victim, the decoupled self-capacitance is  $C_{self}+2C_c$  and the self-inductance is  $L_{self}-L_m$ .

As shown in Fig. 6(a), each bit line can behave as an aggressor and as a victim. The behavior of the aggressor and victim is modeled where the  $i$ th TSV is the victim of the  $(i-1)$ th TSV and the aggressor of the  $(i+1)$ th TSV. As capacitive coupling decays quickly with distance, there is a time skew between the induced noise along a farther refugee and a nearer refugee (see Fig. 6(b)), known as coupling skew [16]. For a non-swizzled eight bit data bus, the capacitance and inductance of each bit line are expressed as

$$L_0 = L_{self} + L_{m1} + L_{m2} + L_{m3} + L_{m4} + L_{m5} + L_{m6} + L_{m7}, \quad (1)$$

$$L_1 = L_{self} + L_{m2} + L_{m3} + L_{m4} + L_{m5} + L_{m6}, \quad (2)$$

$$L_2 = L_{self} + L_{m3} + L_{m4} + L_{m5}, \quad (3)$$

$$L_3 = L_{self} + L_{m4}, \quad (4)$$

$$L_4 = L_{self} - L_{m4}, \quad (5)$$

$$L_5 = L_{self} - L_{m5} - L_{m4} - L_{m3}, \quad (6)$$

$$L_6 = L_{self} - L_{m6} - L_{m5} - L_{m4} - L_{m3} - L_{m2}, \quad (7)$$

$$L_7 = L_{self} - L_{m7} - L_{m6} - L_{m5} - L_{m4} - L_{m3} - L_{m2} - L_{m1}, \quad (8)$$

$$C_0 = C_{self}, \quad (9)$$

$$C_1 = C_2 = C_3 = C_4 = C_5 = C_6 = C_7 = C_{self} + 2C_c, \quad (10)$$

where  $L_i$  and  $C_i$  are, respectively, the inductance and capacitance of the  $i$ th bit line after decoupling.  $L_{mi}$  is the mutual inductance where the separation between two bit lines is  $i$  (in terms of the TSV diameter).

The primary goal of swizzling is to avoid the situation of a worst case victim bit line that affects the efficiency of the entire data bus, both speed and data accuracy. To evenly distribute the influence of an aggressor, each victim bit line is placed nearest to the aggressor once and removed. To make the impedance of each victim ( $v$ ) and refugee line ( $r_1, r_2, r_3, r_4, r_5, r_6$ ) the same, at least seven layers are required (for an eight bit data bus) to perform swizzling six times and obtain the same impedance. As the capacitance of each victim is the same after swizzling [19,20], the problem becomes achieving an equal distribution of the mutual inductance. As shown in Table 1, the total inductance of each victim signal path remains the same, namely,  $L_1 + L_2 + L_3 + L_4 + L_5 + L_6 + L_7$ .

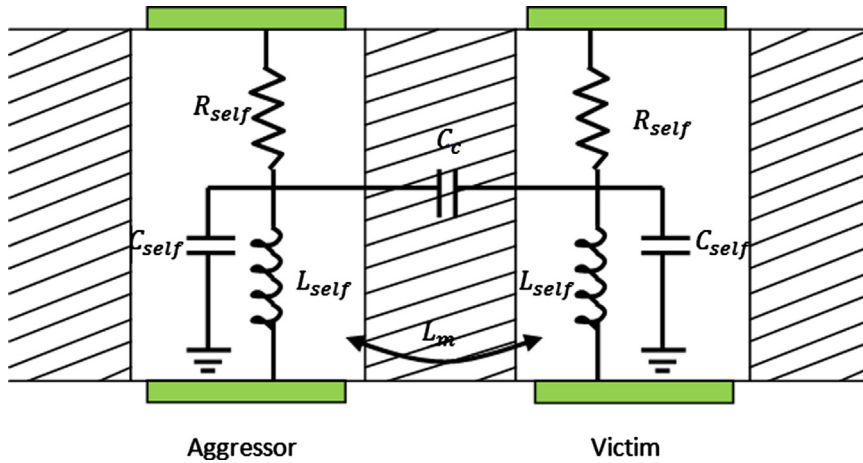


Fig. 4. Model of TSV coupling impedances.

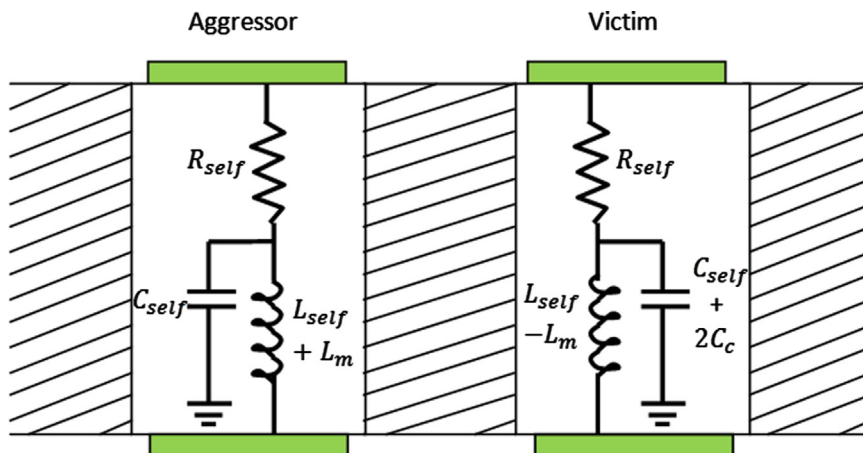


Fig. 5. Decoupled TSVs.

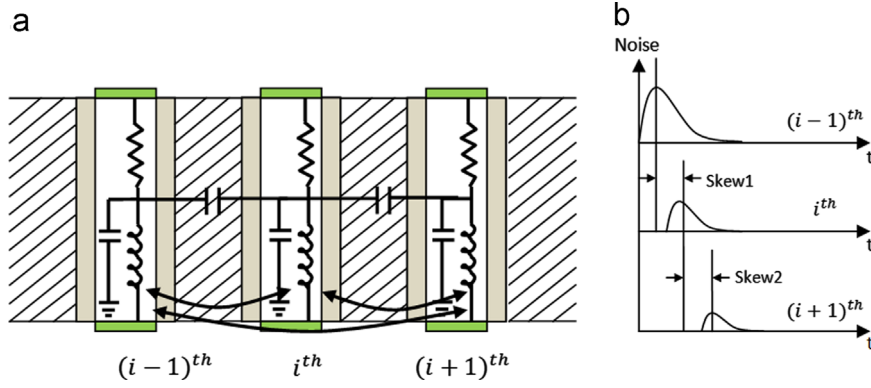


Fig. 6. Coupling skew in TSV-based 3-D data bus: (a) coupling among three adjacent TSVs; and (b) coupling skew of three adjacent TSVs.

**Table 1**  
Distribution of inductance of victim and refugees in a seven layer 3-D IC.

	$\nu$	$r_1$	$r_2$	$r_3$	$r_4$	$r_5$	$r_6$
Layer 1	L1	L2	L3	L4	L5	L6	L7
Layer 2	L2	L3	L4	L5	L6	L7	L1
Layer 3	L3	L4	L5	L6	L7	L1	L2
Layer 4	L4	L5	L6	L7	L1	L2	L3
Layer 5	L5	L6	L7	L1	L2	L3	L4
Layer 6	L6	L7	L1	L2	L3	L4	L5
Layer 7	L7	L1	L2	L3	L4	L5	L6

$\nu$  is the victim,  $r_i$  is the  $i$ th refugee.

Assume the pitch between two adjacent bit lines is  $p$ , and the height of a TSV is  $h$  for an  $n$ -bit data bus in an  $m$ -layer 3-D IC. With the proposed swizzling pattern, the horizontal length of each bit line is  $(n-2) \times p$  and the vertical length is  $m \times h$ . As the length of the horizontal line is small, the horizontal impedance is considered as resistive.

$$Z_{horizontal} = (n-2)pw\rho_{\square}, \quad (11)$$

where  $w$  is the width of the horizontal interconnect, and  $\rho_{\square}$  is the resistivity per unit area.

There are primarily five types of impedances characterizing the vertical portion of a TSV data bus: self-resistance  $R_{self}$ , self-capacitance  $C_{self}$ , self-inductance  $L_{self}$ , coupling capacitance  $C_{coupling}$ , and mutual inductance  $L_{mutual}$ . Closed-form expressions characterizing these parameters have been developed [21]. Based on (1)–(10) and (A.1)–(A.14), the impedance

$$Z_{vertical} = R_{self}m + j\omega C_{line} + \frac{1}{j\omega L_{line}}, \quad (12)$$

where  $C_{line} = (C_{self} + 2C_{coupling})m$ . To apply the optimal swizzling pattern,  $m$  is assumed to be equal to  $n-1$ . The mutual inductance is frequency and distance dependent. When the frequency is fixed, the mutual inductance can be described as  $L_m(i)$ , where  $i$  is the distance (in terms of the number of pitches) between two bit lines. The inductance of each bit line is

$$L_{line} = mL_{self} - (L_m(1) + L_m(2) + L_m(3) + \dots + L_m(m-1) + L_m(m)). \quad (13)$$

The ratio of the horizontal and vertical impedance  $ratio_{impedance}$  is therefore

$$ratio_{impedance} = \frac{|Z_{horizontal}|}{|Z_{vertical}|} = \frac{(n-2)pw\rho_{\square}}{\sqrt{R_{self}^2 m^2 + (2\pi f C_{line} - 1/2\pi f L_{line})^2}} \quad (14)$$

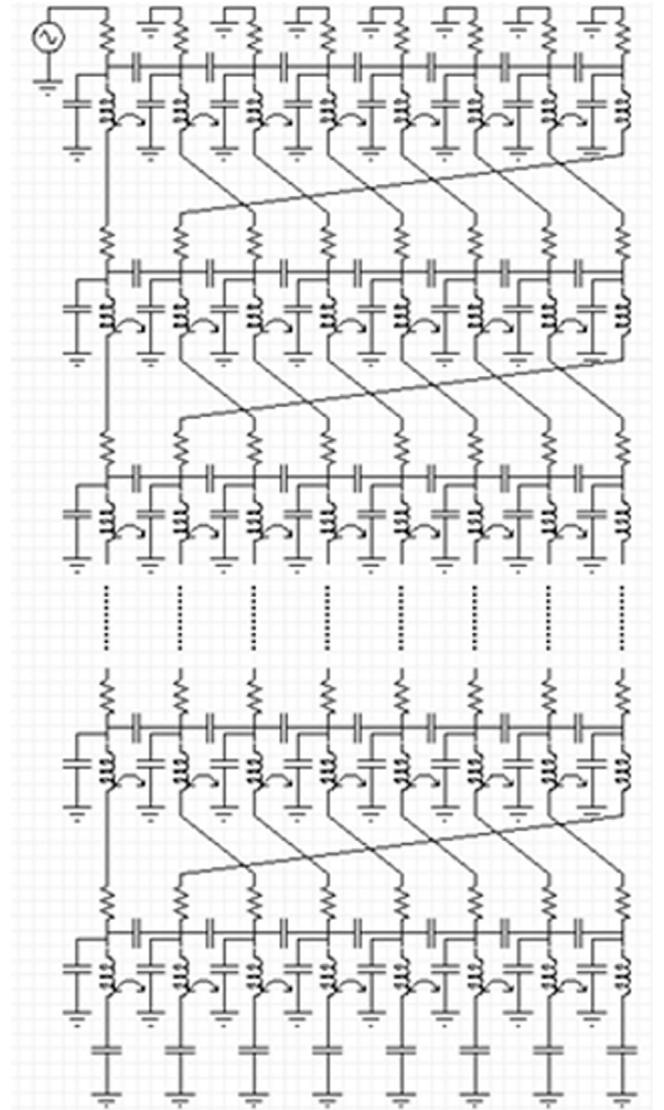


Fig. 7. HSPICE circuit model of an eight bit data bus.

### 3. Demonstration of swizzling

Swizzling is a *conditionally* efficient method for reducing peak coupling noise in a TSV-based 3-D data bus, which depends upon the (a) TSV diameter ( $D$ ), (b) TSV aspect ratio ( $AR$ ), (c) TSV pitch ( $P$ ), and (d) transition time ( $TR$ ) of the aggressor signal. The efficiency



is characterized by a reduction in the peak coupling noise due to swizzling as compared to no swizzling. The parameter setup is described in Section 3.1. The swizzling efficiency for different TSV diameters and aspect ratios is discussed in Section 3.2. The swizzling efficiency for different TSV pitches is introduced in Section 3.3. The swizzling efficiency for different transition times of the aggressor signal is discussed in Section 3.4. The analysis of swizzling optimality is described in Section 3.5.

### 3.1. Parameter setup

The simulation environment utilizes an HSPICE circuit model of an eight bit TSV data bus, as shown in Fig. 7. The aggressor is a ramp signal located at the edge while the other bit lines are grounded. When the aggressor is located in the middle of a data bus, the bit lines can be divided into two groups, with the aggressor at the edge of each group. The methodology is applied to both groups. The TSV diameters (1  $\mu\text{m}$ , 5  $\mu\text{m}$ , 10  $\mu\text{m}$ , 20  $\mu\text{m}$ ,

30  $\mu\text{m}$ ,..., 90  $\mu\text{m}$ , 100  $\mu\text{m}$ ), aspect ratios (5, 10, 15, 20, 25, 30, 35, 40), separations (0.5D, D, 1.5D, 2D, 2.5D, 3D, 3.5D, 4D, 4.5D, 5D), and transition times (10 ps, 20 ps, 30 ps, ..., 80 ps, 90 ps, 100 ps) of the signal on the aggressor, modeled as a ramp, are evaluated.

Determination of the TSV self-resistance, self-capacitance, self-inductance, coupling capacitance, and mutual inductance is based on [21]. The peak coupling noise is measured when the ramp signal switches from 0 V to 1.8 V. The load of each signal path is a capacitor with a value of 10 fF.

### 3.2. Swizzling efficiency for different TSV diameters and aspect ratios

Four different structures of a TSV-based data bus are evaluated: optimal swizzling pattern, swizzling pattern I, swizzling pattern II, and no swizzling, as shown in Fig. 8. As compared to the other three structures, optimal swizzling exhibits the smallest inductance of a signal path, as listed in Table 2. The reduction in peak coupling noise due to swizzling, as compared to no swizzling for different diameters

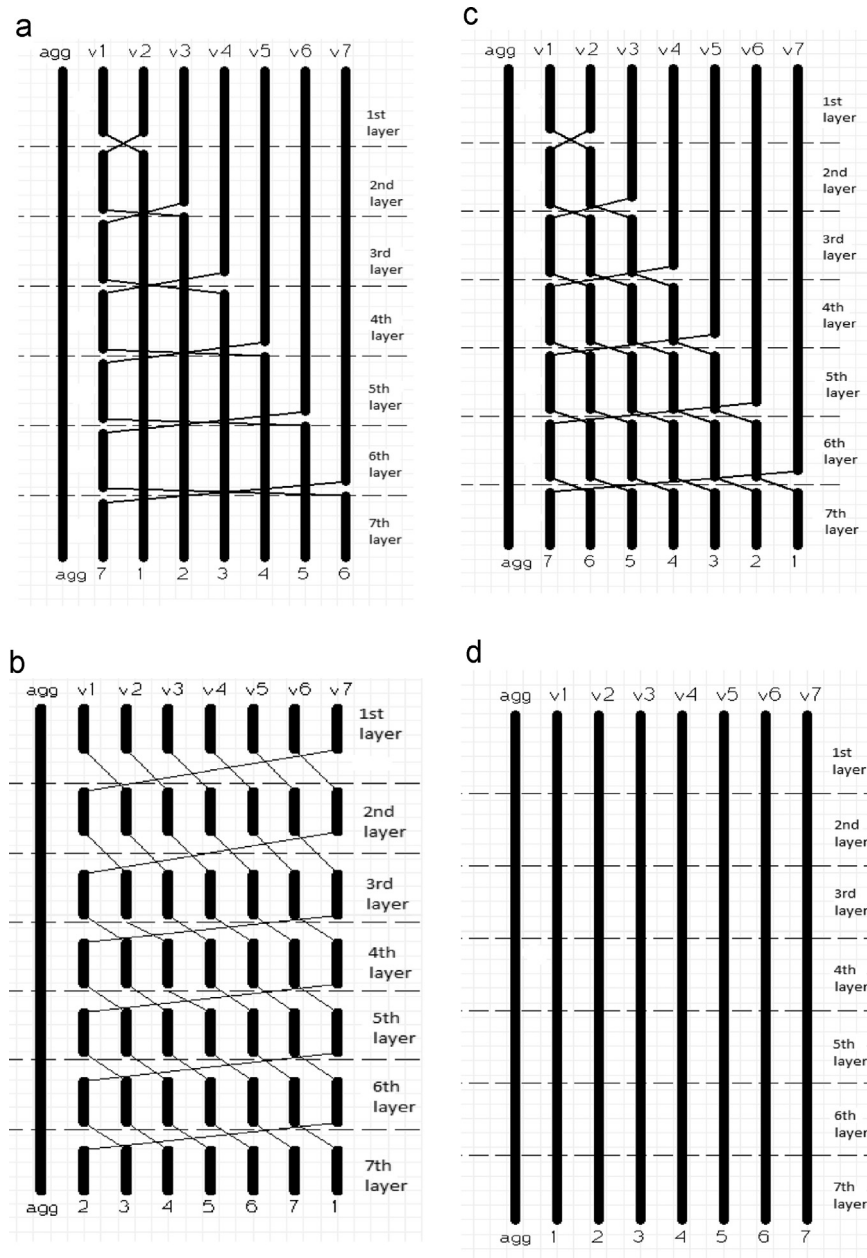


Fig. 8. Structure of TSV-based data bus: (a) swizzling pattern I (P1); (b) optimal swizzling pattern (OP); (c) swizzling pattern II (P2); and (d) no swizzling (no).

and aspect ratios, is listed in Table 3 and shown in Fig. 9. The aggressor transition time is 10 ps.

The peak coupling noise is characterized by  $R$ ,  $L_m$ , and  $C_c$ . With a constant diameter, if the aspect ratio is smaller than 15,  $L_m$  and  $C_c$  are small while  $R$  is large. The peak coupling noise primarily depends upon the resistance  $R$ . When the aspect ratio is larger than 15,  $L_m$  and  $C_c$  become large, and the peak coupling noise is primarily determined by  $L_m$  and  $C_c$ . As the nature of optimal swizzling is to minimize the maximum parasitic coupling impedance, the efficiency of optimal swizzling in reducing the peak coupling noise is higher when the mutual inductance and coupling capacitance are large. The optimal swizzling pattern therefore occurs when the aspect ratio is significant, as exemplified by an aspect ratio larger than 15 when the diameter is 20  $\mu\text{m}$ , as noted in Table 3.

When the TSV diameter is smaller than 5  $\mu\text{m}$ , the impedance of the signal path is primarily resistive. A significant noise is

produced by the small current induced by the aggressor. The high sensitivity of the noise to this induced current affects the noise level, which explains the uncertainty in the swizzling efficiency when the diameter is small (see Fig. 9(a) where the TSV diameter is 1  $\mu\text{m}$ ). When the diameter is larger than 5  $\mu\text{m}$ , the resistance is less significant as compared to the mutual inductance and coupling capacitance. As exemplified in Fig. 9(c), where the TSV diameter is 10  $\mu\text{m}$ , the efficiency of swizzling exhibits a nonlinear relationship with the aspect ratio ( $AR$ ). When the  $AR$  is smaller than ten, the efficiency increases with higher  $AR$ . When the  $AR$  is larger than ten but smaller than 30, the efficiency decreases with  $AR$ . When the  $AR$  is larger than 30, swizzling is inefficient in all cases.

This nonlinear trend, illustrated in Fig. 9, can be explained by the coupling skew. The magnitude of the decoupled capacitance depends upon the signals on the lines. As listed in Table 4, for an aggressor and a quiet victim, the decoupled victim capacitance is  $C + 2C_c$ ; for an aggressor and victim with the same phase, the decoupled victim capacitance is  $C$ ; for an aggressor and victim with the opposite phase, the decoupled victim capacitance is  $C + 4C_c$  [16,22]. Due to the coupling skew, the phase difference varies between the signals on adjacent lines. As exemplified in Fig. 9(c), when the  $AR$  is less than ten, the amplitude of the induced coupling noise is low due to the small coupling impedance. Two adjacent bit lines can be modeled as an aggressor and a quiet victim. The equal distribution of the mutual impedances is not significantly affected. Hence, swizzling lowers the maximum noise. However, with increasing  $AR$ , the coupled noise on each bit line increases with higher coupling impedance. The previously

**Table 2**  
Maximum inductance of the four swizzling patterns.

Pattern	Maximum inductance	Comparison
Optimal swizzling	$L_{op} = 7L_{self} - L_{m7} - L_{m6} - L_{m5} - L_{m4} - L_{m3} - L_{m2} - L_{m1}$	$L_{op} < L_{p2} < L_{p1} < L_{no}$
Swizzling pattern I	$L_{p1} = 7L_{self} + L_{m2} + 7L_{m3} + 7L_{m4} + 7L_{m5} + L_{m6}$	
Swizzling pattern II	$L_{p2} = 7L_{self} + L_{m2} + L_{m3} + 3L_{m4} + 7L_{m5} + L_{m6}$	
No swizzling	$L_{no} = 7L_{self} + 7L_{m2} + 7L_{m3} + 7L_{m4} + 7L_{m5} + 7L_{m6}$	

**Table 3**  
Reduction in peak coupling noise as compared to no swizzling,  $TR = 10$  ps.

AR/D	1 $\mu\text{m}$			5 $\mu\text{m}$			10 $\mu\text{m}$			20 $\mu\text{m}$		
	P1	P2	Op	P1	P2	Op	P1	P2	Op	P1	P2	Op
5	-0.8	45.0	51.4	13.4	7.8	-2.2	14.2	17.1	5.67	20.9	17.3	9.4
10	-3.1	-7.4	-4.8	3.5	15.8	4.5	12.1	32.7	13.6	18.6	36.6	26.1
15	-6.0	-1.6	0.34	2.8	18.9	23.3	7.0	25.4	27.5	13.7	26.8	11.8
20	0.0	4.9	4.9	2.8	16.0	27.1	7.2	21.6	23	9.6	18.5	25.3
25	-3.7	4.8	5.85	-10.9	7.3	17.7	7.5	17.9	21.6	7.2	13.7	20.9
30	-11.1	-3.0	-1.0	-18.2	0.0	9.0	0.8	10.5	18.5	4.5	11.2	19.4
35	-14.3	-6.7	4.3	-38.1	-15.1	-0.48	-10.5	-1.8	12.6	-4.0	3.2	15.1
40	-30.4	-17.8	-5.2	-57.5	-35.2	-16.9	-44.6	-29.1	-12.6	-21.1	-7.3	7.3
AR/D	30 $\mu\text{m}$			40 $\mu\text{m}$			50 $\mu\text{m}$			60 $\mu\text{m}$		
	P1	P2	Op	P1	P2	Op	Op	P2	Op	P1	P2	Op
5	21.8	23.8	17.7	23.8	28.5	19.2	21.6	24.8	21.2	20.8	24.0	15.7
10	17.9	34.6	19.8	17.2	33.1	19.6	17.5	33.1	21.1	17.4	33.5	21.7
15	14.0	24.8	29.9	14.4	25.6	34.4	14.3	24.8	21.1	15.4	25.3	20.5
20	10.7	18.1	26.2	13.7	20.3	26.8	13.1	20.3	15.8	14.2	21.3	22.2
25	11.1	16.7	20.8	11.0	16.6	31.0	11.0	16.4	18.4	11.6	17.0	16.4
30	7.3	11.7	19	8.6	11.5	27.3	9.9	12.7	16.9	9.9	12.0	15.5
35	0.8	6.8	20	2.2	7.5	23.1	2.9	8.8	18.4	2.2	7.4	18.4
40	-17.1	-4.7	13.23	-11.9	-2.2	16.3	-10.9	-2.2	13.1	-17.4	-7.6	11.7
AR/D	70 $\mu\text{m}$			80 $\mu\text{m}$			90 $\mu\text{m}$			100 $\mu\text{m}$		
	P1	P2	Op	P1	P2	Op	P1	P2	Op	P1	P2	Op
5	23.2	23.9	14.9	23.1	23.7	15.5	23.4	28.5	15.4	21.6	24.8	15.8
10	17.4	32.9	24.6	17.3	33.3	25.7	16.8	32.9	26.8	17.5	33.1	26.9
15	14.2	25.3	21	14.1	25.8	32.1	14.1	25.2	31.3	14.3	24.8	31.3
20	13.5	20.6	22.6	13.0	20.1	22.6	13.5	20.5	21.4	13.1	20.3	21.8
25	12.1	16.8	17	10.8	15.5	16.8	10.8	15.5	17	11.0	16.4	16.9
30	9.2	12.0	15.5	7.7	12.0	15.5	7.7	12.6	16.2	9.9	12.7	17.5
35	1.5	6.6	19.1	4.2	9.1	20.4	6.0	10.7	23.8	2.9	8.8	25.5
40	-23.0	-14.3	6.8	-34.7	-22.0	0.8	-38.8	-25.0	-7.6	-10.9	-2.2	-10.3

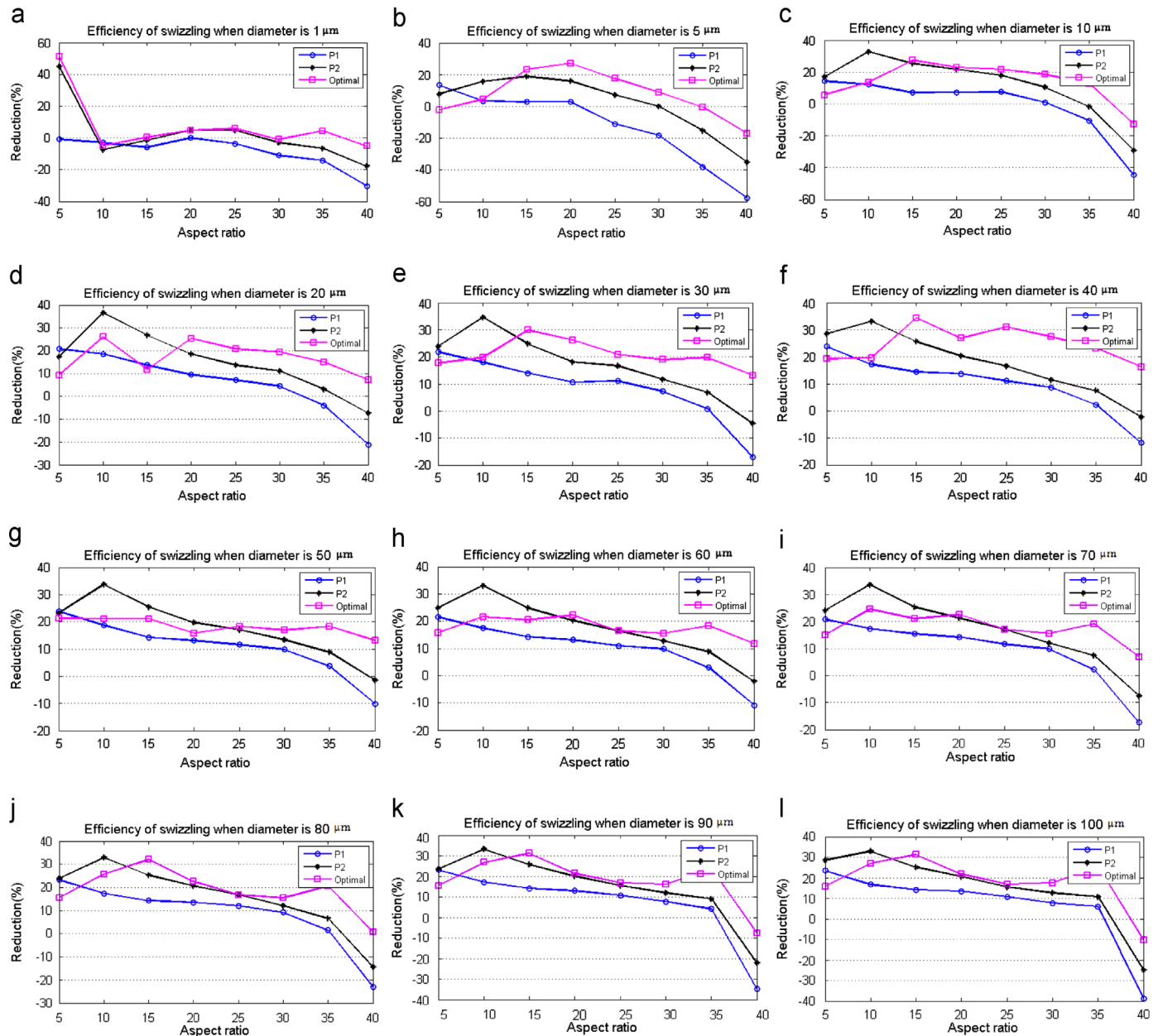


**Fig. 9.** Reduction in peak coupling noise due to swizzling as compared to no swizzling, for TSV diameters: (a) 1  $\mu\text{m}$ ; (b) 5  $\mu\text{m}$ ; (c) 10  $\mu\text{m}$ ; (d) 20  $\mu\text{m}$ ; (e) 30  $\mu\text{m}$ ; (f) 40  $\mu\text{m}$ ; (g) 50  $\mu\text{m}$ ; (h) 60  $\mu\text{m}$ ; (i) 70  $\mu\text{m}$ ; (j) 80  $\mu\text{m}$ ; (k) 90  $\mu\text{m}$ ; and (l) 100  $\mu\text{m}$ .

quiet victim also effectively behaves as an aggressor. The relation of the signal phases along all of the bit lines becomes significantly more complicated. As the decoupled victim capacitance depends upon the signal behavior, the objective of maintaining an equal distribution of the impedance is no longer satisfied. The efficiency of swizzling is therefore reduced.

### 3.3. Swizzling efficiency for different TSV pitches

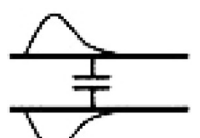
As shown in Fig. 10(b), when the separation between two adjacent TSVs is smaller than twice the diameter ( $2D$ ), the efficiency of swizzling increases with the pitch. When the pitch is larger than twice the diameter ( $2D$ ), the swizzling efficiency decreases. When the bit lines are near to each other, namely, the separation is smaller than  $2D$ , both the adjacent and non-adjacent coupling is significant. The large parasitic impedance leads to significant coupling skew which violates the optimality objective of an equal impedance distribution. With increasing pitch,

non-adjacent inductive coupling becomes less significant. The influence of coupling skew on the impedance distribution is weaker and the swizzling efficiency increases. When the pitch is greater than  $2D$ , both the adjacent and non-adjacent inductive coupling is negligible. The coupling noise becomes small while the reduction in noise due to swizzling is reduced. The swizzling efficiency therefore decreases.

### 3.4. Swizzling efficiency for different transition times of aggressor signal

The swizzling efficiency for different aggressor transition times can be stated as follows: the shorter the transition time, the greater the reduction in peak coupling noise, as listed in Table 5 and shown in Fig. 11. Faster signal transitions produce a larger coupling noise due to a larger  $(d_v/d_t)$  or  $(d_v/d_t)$ . Each signal path operates as a series of distributed low pass RC filters [23]. As the impedance parameters do not change with different transition times, the cut-off frequency of

**Table 4**  
Decoupled victim capacitance with different signals [22].

Description			
Situation	An aggressor, quiet victim	Same phase	Opposite phase
Decoupled victim capacitance	$C+2C_c$	$C$	$C+4C_c$

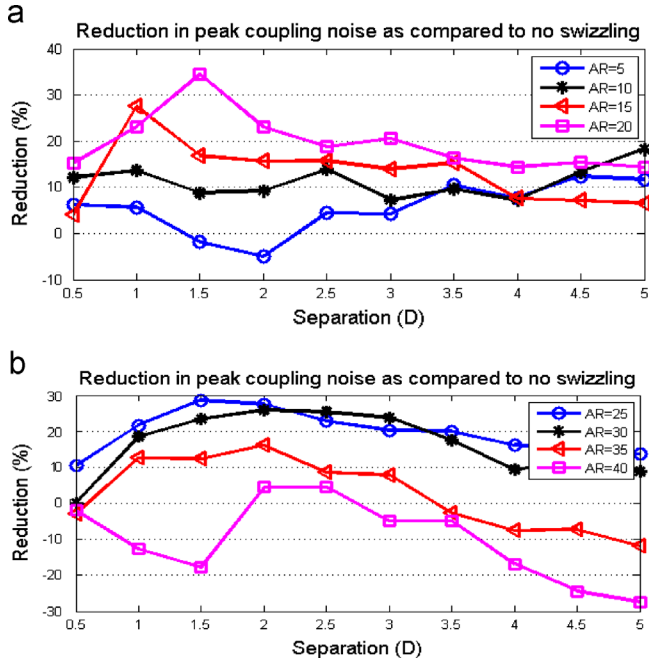


**Fig. 10.** Efficiency of swizzling for different TSV pitches: (a) aspect ratio is 5, 10, 15, and 20, and (b) aspect ratio is 25, 30, 35, and 40.

each signal path remains the same. The noise at the output of the data bus is therefore the same. Hence, the reduction is larger for a fast transition time than a slow transition time. Special cases appear when the aspect ratio is smaller than 20 (see Fig. 11(a)), where the swizzling efficiency increases since the transition time is larger than 70 ps. With a decreasing aspect ratio, parameters such as the resistance, mutual inductance, and coupling capacitance become smaller. A slow transition time produces less coupling noise. A low noise voltage exhibits a higher sensitivity to adjacent and non-adjacent coupling. The input noise for a slow transition time can therefore be greater than a fast transition time. As the output of the distributed RC filters does not change, the efficiency of swizzling increases despite a slower transition time when the aspect ratio is low.

### 3.5. Optimality analysis

The optimal swizzling pattern is a *conditionally* efficient method for reducing peak coupling noise in TSV-based 3-D data buses. As listed in Table 6, OP stands for the optimal swizzling pattern, P1 represents swizzling pattern one, P2 represents swizzling pattern two, and NO means no swizzling. The optimality of the proposed swizzling pattern is observed with large TSVs, where the aspect ratio is larger than 15. The peak coupling noise is dependent on the resistance  $R$ , mutual inductance  $L_{mutual}$ , and

**Table 5**  
Reduction in peak coupling noise as compared to no swizzling,  $D=10\ \mu\text{m}$ .

TR/AR	5			10			15			20		
	P1	P2	OP	P1	P2	OP	P1	P2	OP	P1	P2	OP
10 ps	14	17	6	12	33	14	7	25	27	7	22	23
20 ps	14	10	-5	12	24	6	7	24	22	8	21	22
30 ps	-5	4	-12	13	19	-4	9	17	11	6	19	25
40 ps	12	16	19	11	14	-8	8	13	2	3	11	15
50 ps	10	5	-10	6	6	-17	8	10	-3	6	9	8
60 ps	1	-7	-39	3	-2	-13	2	4	-9	5	5	4
70 ps	-11	1	-21	7	9	6	-12	-13	-20	-4	-3	1
80 ps	-20	-4	-6	21	27	32	-12	-11	-14	-13	-12	-5
90 ps	26	20	20	13	18	18	-6	-5	2	-21	-20	-12
100 ps	24	26	0	20	20	11	-2	1	13	-14	-13	-2
TR/AR	25			30			35			40		
%	P1	P2	OP	P1	P2	OP	P1	P2	OP	P1	P2	OP
10 ps	7	18	22	1	10	19	-11	-2	13	-45	-29	-13
20 ps	0	14	17	-4	10	15	-10	4	10	-48	-26	-17
30 ps	1	14	20	-3	10	17	-16	0	7	-57	-38	-19
40 ps	-2	9	18	-6	5	15	-21	-7	5	-61	-45	-23
50 ps	1	5	10	-7	-1	13	-21	-12	5	-59	-48	-28
60 ps	1	2	2	-6	-2	5	-11	-6	2	-50	-48	-31
70 ps	-1	1	5	1	-1	7	-5	-7	0	-47	-48	-37
80 ps	-15	-14	-6	-13	-11	-2	-10	-8	-2	-48	-56	-41
90 ps	-25	-22	-12	-21	-16	-4	-23	-19	-8	-50	-59	-37
100 ps	-27	-24	-9	-31	-28	-9	-33	-33	-13	-49	-58	-30

coupling capacitance  $C_{coupling}$ . The peak coupling noise is primarily dependent on the resistance  $R$ . When the aspect ratio is larger than 15,  $L_{mutual}$  and  $C_{coupling}$  are large and exceed the influence of the resistance on coupling noise. The impedance of each decoupled signal path can be minimized by utilizing the optimal swizzling pattern, where the influence of  $L_{mutual}$  and  $C_{coupling}$  on the peak coupling noise is reduced. The optimality of our swizzling pattern is observed when the TSV aspect ratio is greater than 15.

## 4. Conclusions

Swizzling is a *conditionally* efficient method for reducing peak coupling noise in TSV-based 3-D data buses. An optimal swizzling pattern is proposed based on an analysis of the parasitic coupling impedance. The optimality is demonstrated through HSPICE simulations which consider different TSV diameters, aspect ratios, pitches, and transition times of the aggressor, as compared to no swizzling and two other swizzling patterns. A maximum 51% reduction in peak coupling noise is achieved.

The proposed optimal swizzling pattern assumes that the edge line of a data bus is the aggressor line which propagates the fastest transition signal. As the least significant bit (LSB), which is the



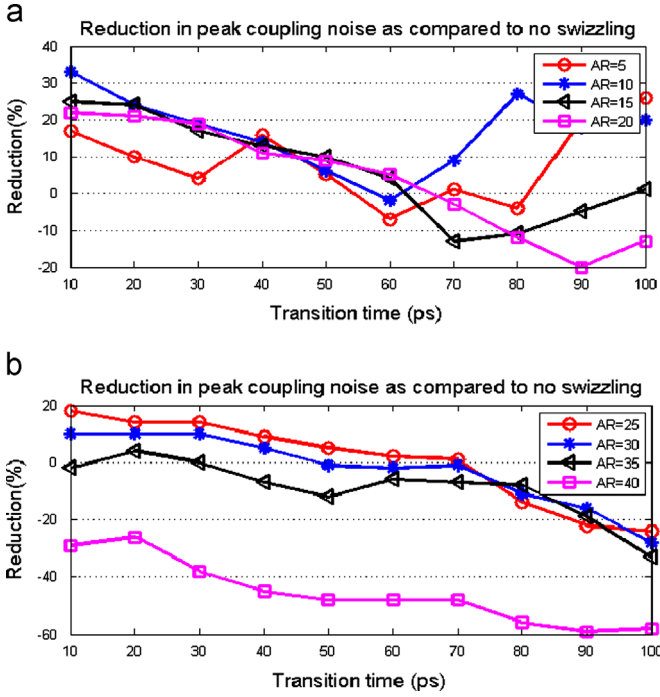


Fig. 11. Efficiency of swizzling for different transition times of the aggressor: (a) aspect ratio is 5, 10, 15, and 20, and (b) aspect ratio is 25, 30, 35, and 40.

Table 6  
Swizzling pattern for different TSV diameters and aspect ratios.

TSV	$D$ ( $\mu\text{m}$ )/AR	5	10	15	20	25	30	35	40
Thin	1	OP	NO	OP	P2/OP	OP	NO	NO	NO
	5	P1	P2	OP	OP	OP	OP	NO	NO
Bulk	10	P2	P2	OP	OP	OP	OP	OP	NO
	20	P1	P2	P2	OP	OP	OP	OP	OP
	30	P2	P2	OP	OP	OP	OP	OP	OP
	40	P2	P2	OP	OP	OP	OP	OP	OP
	50	P2	P2	P2	P2	OP	OP	OP	OP
	60	P2	P2	P2	P2	OP	OP	OP	OP
	70	P2	P2	P2	OP	P2/OP	OP	OP	OP
	80	P2	P2	P2	OP	OP	OP	OP	OP
	90	P2	P2	OP	OP	OP	OP	OP	NO
	100	P2	P2	OP	OP	OP	OP	OP	NO

OP: optimal swizzling pattern; P1: swizzling pattern one; P2: swizzling pattern two; NO: no swizzling.

edge line of a data bus, generally exhibits the greatest switching, it is reasonable to assume the fastest transition signal propagates along the edge line. As shown in Fig. 12, when the aggressor signal propagates along a middle bit line, the bit lines of a data bus can be divided into two groups, with the aggressor line residing at the edge of each of the groups. The situation in each group becomes the same as the situation discussed in the previous section. The proposed optimal swizzling method can therefore be applied in a data bus where the aggressor is located between edges.

For a wider application of the proposed methodology in determining the optimal swizzling pattern, several shortcomings need to be overcome; specifically, the largest number of swizzling events should not be constrained by the number of layers within a 3-D IC, the swizzling pattern should be uniform for different input signals, and non-negligible horizontal impedance as compared to the vertical impedance should be considered. All of these issues require further study.

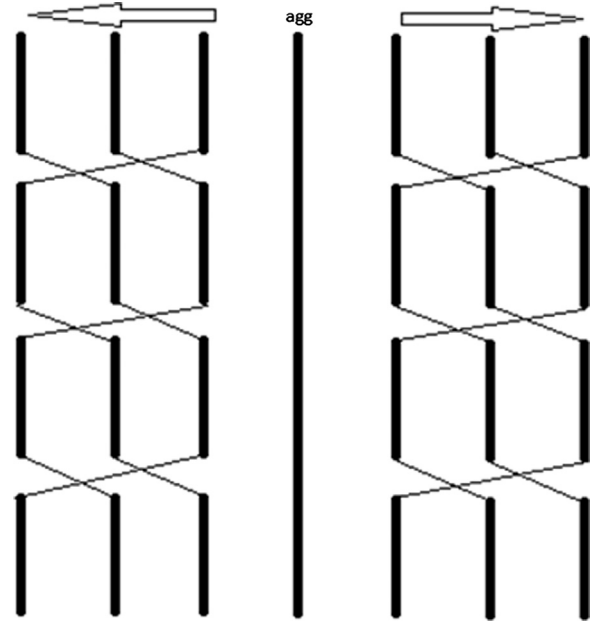


Fig. 12. Swizzling pattern when the aggressor is not at either edge.

## Appendix A. Closed-form expressions for TSV resistance, capacitance, and inductance

Closed-form expressions characterizing the self-resistance  $R_{self}$ , self-capacitance  $C_{self}$ , self-inductance  $L_{self}$ , coupling capacitance  $C_{coupling}$ , and mutual inductance  $L_{mutual}$  are summarized in (A.1)–(A.14) [21].

$$R_{self} = \frac{1}{\sigma_w} \frac{L}{\pi R^2}, \quad (\text{A.1})$$

where  $R$  is the radius of a TSV and  $L$  is the length of a TSV.  $\sigma_w$  is the conductivity of the filled materials.

$$\alpha = \begin{cases} 1 - e^{-4.3L/D} & \text{if } f = DC, \\ 0.94 + 0.52e^{-10|f/b-1|} & \text{if } f > f_{asym}, \end{cases} \quad (\text{A.2})$$

where  $f_{asym}$  is within the intermediate frequency zone, 200–800 MHz [21], when the self-inductance of a TSV begins to decrease.

$$\beta = \begin{cases} 1 & \text{if } f = DC, \\ 0.1535 \ln \frac{L}{D} + 0.592 & \text{if } f > f_{asym}, \end{cases} \quad (\text{A.3})$$

$$DC : \begin{cases} L_{self} = \alpha \frac{\mu_0}{2\pi} \left[ \ln \left( \frac{L + \sqrt{L^2 + R^2}}{R} \right) L + R - \sqrt{L^2 + R^2} + \frac{L}{4} \right] \\ L_{mutual} = \beta \frac{\mu_0}{2\pi} \left[ \ln \left( \frac{L + \sqrt{L^2 + P^2}}{P} \right) L + P - \sqrt{L^2 + P^2} \right], \end{cases} \quad (\text{A.4})$$

$$f_{asym} : \begin{cases} L_{self} = \alpha \frac{\mu_0}{2\pi} \left[ \ln \frac{2L}{R} - 1 \right] L \\ L_{mutual} = \beta \frac{\mu_0}{2\pi} \left[ \ln \left( \frac{L + \sqrt{L^2 + P^2}}{P} \right) L + P - \sqrt{L^2 + P^2} \right], \end{cases} \quad (\text{A.5})$$

$\alpha$  and  $\beta$ , used in (A.4) and (A.5), are provided, respectively, in (A.2) and (A.3).  $t_0$  is the thickness of the barrier and  $S$  is the separation of two adjacent TSVs. The TSV pitch  $P$  is expressed as  $P = S + 2(R + t_0)$ .

$$C_{self} = \alpha \beta \frac{\epsilon_{SiO_2}}{t_{diel} + (\epsilon_{SiO_2}/\epsilon_{Si})x_d T_p} 2\pi RL, \quad (\text{A.6})$$

$$x_d T_p = \sqrt{\frac{4\epsilon_{Si}\phi_f p}{qN_A}}, \quad (\text{A.7})$$

$$\varphi_{f_p} = V_{th} \ln \left( \frac{N_A}{n_i} \right), \quad (\text{A.8})$$

$$\alpha = \left( -0.0351 \frac{L}{D} + 1.5701 \right) S_{gnd,\mu m}^{0.0111(L/d)-0.1997}, \quad (\text{A.9})$$

$$\beta = 5.8934 D_{\mu m}^{-0.553} \left( \frac{L}{D} \right)^{-(0.0031 D_{\mu m} + 0.43)}. \quad (\text{A.10})$$

$\alpha$  and  $\beta$ , used in (A.6), are provided in (A.9) and (A.10).  $x_{dT_p}$  is the depletion region depth,  $\varphi_{f_p}$  is the p-type silicon work function, and  $N_A$  is the doped acceptor concentration with a value of  $10^{21} \text{ m}^{-3}$ .  $n_i$  is the intrinsic semiconductor concentration with a value of  $1.5 \times 10^{16} \text{ m}^{-3}$ . The thermal voltage  $V_{th}$  is  $(kT/q)$ . When  $T=300 \text{ K}$ , the value is  $25.9 \text{ mV}$ . The silicon permittivity is  $11.7 \times 8.85 \times 10^{-12} \text{ F/m}$  and the permittivity of  $\text{SiO}_2$  is  $3.9 \times 8.85 \times 10^{-12} \text{ F/m}$ .  $t_{diel}$  is the thickness of the dielectric, which is assumed to be  $100 \text{ nm}$ .  $S_{gnd}$  is assumed to be  $10 \mu\text{m}$ , the distance of a TSV to the ground plane.

$$C_{coupling} = 0.4\alpha\beta\gamma \cdot \frac{\epsilon_{Si}}{S} \pi DL, \quad (\text{A.11})$$

$$\alpha = 0.225 \ln \left( 0.97 \frac{L}{D} \right) + 0.53, \quad (\text{A.12})$$

$$\beta = 0.5711 \left( \frac{L}{D} \right)^{-0.988} \ln(S_{gnd,\mu m}) + (0.85 - e^{-(L/D)+1.3}), \quad (\text{A.13})$$

$$\gamma = 1 \quad (\text{A.14})$$

$\alpha$ ,  $\beta$  and  $\gamma$ , used in (A.11), are provided, respectively, in (A.12), (A.13) and (A.14).

## References

- [1] Y. Akasaka, Three-dimensional IC trends, Proc. IEEE 74 (12) (1986) 1703–1714.
- [2] J.L. Hennessy, D.A. Patterson, Computer Architecture: A Quantitative Approach, Burlington, Massachusetts, Morgan Kaufmann, 2007.
- [3] M. Daraban, Statistical information of crosstalk on parallel bus, in: Proceedings of the IEEE International Symposium for Design and Technology in Electronic Packaging, October 2011, pp. 211–216.
- [4] M. Favalli, L. Benini, Analysis of glitch power dissipation in CMOS ICs, in: Proceedings of the IEEE International Symposium on Low Power Design, April 1995, pp. 123–128.
- [5] V.F. Pavlidis, E.G. Friedman, Three-Dimensional Integrated Circuit Design, Burlington, Massachusetts, Morgan Kaufmann, 2009.
- [6] X. Gui, Three-dimensional thermal analysis of high density triple-level interconnection structures in very large scale integrated circuits, J. Vac. Sci. Technol. B: Microelectron. Nanometer Struct. 12 (1994) 59–62.
- [7] E. Todorovich, E. Boemo, Statistical power estimation for FPGA's, in: Proceedings of the IEEE International Conference on Field Programmable Logic and Applications, August 2005, pp. 515–518.
- [8] B. Kahng, S. Muddu, E. Sarto, Interconnect optimization strategies for high-performance VLSI designs, in: Proceedings of the IEEE International Conference on VLSI Design, January, 1999, pp. 464–469.
- [9] K.M. Lepak, I. Luwandu, L. He, Simultaneous shield insertion and net ordering for coupled RLC nets under explicit noise constraint, in: Proceedings of the IEEE Design Automation Conference, June 2001, pp. 199–202.
- [10] M.M. Ghoneima, Y. Ismail, Skewed repeater bus: a low-power scheme for on-chip buses, IEEE Trans. Circuits Syst. I: Regular Pap. 55 (7) (2008) 1904–1910.
- [11] L.J. Herbst, A critical look at interconnect scaling, in: Proceedings of the IEEE Colloquium on New Directions in VLSI Design, November 1989, pp. 9.1–9.6.
- [12] S. Kose, E. Salman, E.G. Friedman, Shielding methodologies in the presence of power/ground noise, IEEE Trans. Very Large Scale Integration Syst. 19 (8) (2011) 1458–1468.
- [13] S.M. Alam, Inter-strata connection characteristics and signal transmission in three-dimensional (3D) integration technology, in: Proceedings of the IEEE International Symposium on Quality Electronic Design, March 2007, pp. 580–585.
- [14] V.F. Pavlidis, E.G. Friedman, Interconnect-based design methodologies for three-dimensional integrated circuits, Proc. IEEE 97 (1) (2009) 123–140.
- [15] W.A. Davis, K.K. Agarwal, Radio Frequency Circuit Design, New York City, New York, Wiley, 2011.
- [16] B. Soudan, Reducing mutual inductance of wide signal busses through swizzling, in: Proceedings of the IEEE International Conference on Electronics, Circuits and Systems, vol. 2, 14–17 December 2003, pp. 870–873.
- [17] B. Soudan, Controlling inductive coupling in wide global signal busses through swizzling, Analog Integrated Circuits Signal Process. 43 (2) (2005) 191–203.
- [18] K.T. Tang, E.G. Friedman, Interconnect coupling noise in CMOS VLSI circuits, in: Proceedings of the ACM International Symposium on Physical Design, April 1999, pp. 48–53.
- [19] J. Zhang, E.G. Friedman, Decoupling technique and crosstalk analysis of coupled RLC interconnects, in: Proceedings of the IEEE International Symposium on Circuits and Systems, vol. II, May 2004, pp. 521–524.
- [20] J. Zhang, E.G. Friedman, Crosstalk modeling for coupled RLC interconnects with application to shield insertion, IEEE Trans. Very Large Scale Integration (VLSI) Syst. 14 (6) (2006) 641–646.
- [21] I. Savidis, E.G. Friedman, Closed-form expressions of 3-D via resistance, inductance, and capacitance, IEEE Trans. Electron. Dev. 56 (9) (2009) 1873–1881.
- [22] K.T. Tang, E.G. Friedman, Delay and noise estimation of CMOS logic gates driving coupled resistive–capacitive interconnections, Integration, VLSI J. 29 (2) (2000) 131–165.
- [23] C.K. Alexander, M.N. Sadiku, Fundamentals of Electric Circuits, Third Edition, New York City, New York, McGraw-Hill, 2007.